PROCEEDINGS OF SCIENCE

Characterization of Charge Spreading and Gain in Encapsulated Resistive Micromegas Detectors for the T2K-TPC

Samira Hassani[a,*] **and Jean-François Laporte**[a] **for the HA-TPC group**

[a] *IRFU, CEA, Université Paris-Saclay, Gif-sur-Yvette, France*

E-mail: samira.hassani@cea.fr, jean-francois.laporte@cea.fr

The near detector of the T2K experiment has recently undergone a major upgrade. New Time Projection Chambers have been constructed, based on the innovative resistive Micromegas technology. A resistive layer is deposited onto the segmented anode in order to spread the charge onto several adjacent pads. This way, the spatial resolution for a given segmentation is improved. The results of the first detailed characterization of the charge spreading in resistive Micromegas detectors will be presented. A detailed physical model has been developed to describe the charge dispersion phenomena in the resistive Micromegas anode. The detailed physical description includes initial ionization, diffusion effects and the readout electronics response, including description and simulation of noise. The model provides an excellent characterization of the charge spreading of the experimental measurements and allowed the simultaneous extraction of gain and *RC* information of the modules.

42nd *International Conference on High Energy Physics*
18-24 July 2024
Prague, Czech Republic

*Speaker

PoS(ICHEP2024)1063

1. Introduction

The T2K (Tokai to Kamioka) [1] is a long baseline neutrino oscillation experiment in Japan, which conducts measurements of neutrino oscillation parameters by generating a highly intense muon (anti) neutrino beam centered at 600 MeV at the J-PARC facility. This beam is measured 280 m from its point of origin by a set of near detectors (ND280), positioned prior to oscillations, with the aim of monitoring and constraining systematic uncertainties associated with the neutrino flux and interaction models. Subsequently, the far detector, situated an additional 295 km away, is Super-Kamiokande, responsible for detecting the disappearance of muon (anti) neutrinos and the appearance of electron (anti) neutrinos within the beam.

The ND280 has recently undergone an upgrade, which involves the integration of a suite of subdetectors positioned at the upstream section of the existing ND280 setup as shown in Figure 1. This upgraded configuration features a finely segmented active target known as the Super-FGD, positioned between two high angle time projection chambers (HA-TPCs), all enclosed by a time-of-flight detector (ToF). The installation of these new detectors at J-PARC was completed in May 2024, and the first neutrino data were collected during June 2024.

2. Encapsulated Resistive Anode Micromegas

The HA-TPC features new field cage design to minimize dead space and maximize tracking volume. It is equipped with new readout based on the innovative resistive Micromegas technology [2]. Figure 1 illustrates the concept of resistive Micromegas.

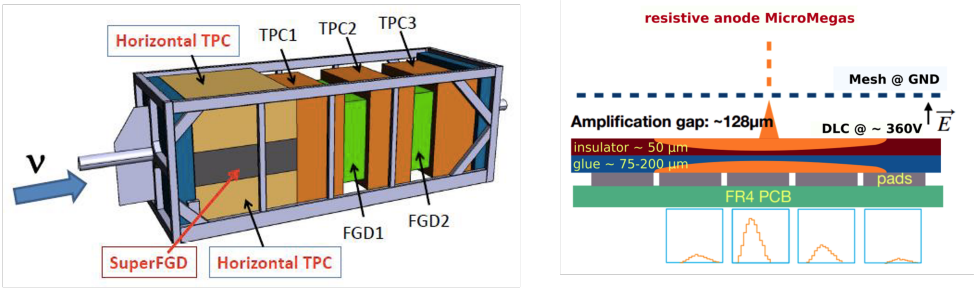

Figure 1: The T2K near detector setup (left) Principle of Resistive Micromegas (right)

In the resistive anode design, charge dispersion is achieved by applying a resistive foil (DLC) over the pad plane. As the initial charge spreads across multiple pads, it allows for improved position resolution without the need to reduce the size of the readout pads, making this a compact and cost-effective technology. The resistive foil on the anode slows down the charge dissipation process, thereby reducing the frequency and intensity of sparks without the need for additional spark protection measures. A novel high-voltage powering scheme is utilized in resistive anode Micromegas operation, where the mesh is grounded, and the anode is set to a positive voltage. This approach enhances the safety of detector handling and improves the uniformity of the electric field. Due to this high-voltage scheme, the current Micromegas design is referred to as Encapsulated Resistive Anode Micromegas, or "ERAM" for short.

The ERAM module consists of a resistive Micromegas detector glued on an aluminium frame on which the readout electronics is fixed directly on its backside. The 42×34 cm^2 detector has 1152 pads of 11.18×10.09 mm^2 disposed in a matrix of 36 pads along x direction and 32 pads along y direction. The pad plane is covered by a resistive layer made of an insulated 50 µm Apical polyimide foil (pressed with 150 µm glue), on which diamond-like carbon (DLC) is deposited by electron beam sputtering.

The successful validation of detector prototypes for the new HA-TPCs has been achieved through several test-beam campaigns at CERN and DESY. These tests have not only confirmed the reliability of the detector technologies but have also provided valuable insights into their performance. A spatial resolution better than 800 µm and a dE/dx resolution better than 10% are measured for all the incident angles and all the drift distances [2].

3. Encapsulated Resistive Anode Micromegas Characterisation

A dedicated X-ray test bench is used to characterize the ERAMs, scanning each pad individually for precise measurements of gain uniformity and energy resolution. The setup consists of an aluminium chamber with 3 cm drift distance and a robotic $x-y-z$ arm system on an optical breadboard of 120×60 cm^2 holding a 280 MBq ^{55}Fe radioactive source. A comprehensive physical model, encompassing aspects like initial ionization, diffusion effects, and readout electronics, characterizes charge dispersion phenomena. This model enables simultaneous extraction of gain and charge spreading information (RC) from the modules.

3.1 Electronics response model

The ERAM readout electronics is based on the AFTER chip [3], operating at a sampling frequency of 25 MHz with a peaking time of either 200 ns or 412 ns. Each ASIC processes 72 electronic channels connected to a 9×8 pad array. A Front End Card (FEC), which accommodates eight AFTER ASICs, handles the digitization of the pad signals. To fully read a single ERAM module, two FECs are required, which are directly mounted onto the detector PCB. When the AFTER chip is fed with a Dirac current pulse $I(t) = Q_{anode}\delta(t)$, its response, prior to late discretization stage is proportional to the function [4]:

$$f(t; w_s, Q) = e^{-w_s t} + e^{-\frac{w_s t}{2Q}} \left[\sqrt{\frac{2Q-1}{2Q+1}} \sin\left(\frac{w_s t}{2}\sqrt{4-\frac{1}{Q^2}}\right) - \cos\left(\frac{w_s t}{2}\sqrt{4-\frac{1}{Q^2}}\right)\right] \quad (1)$$

This function can be equated to the electronics output (in the form of ADC) by means of a proportionality factor as:

$$ADC^D(t; w_s, Q) = \frac{ADC_o}{Q_o}\frac{f(t; w_s, Q)}{f_{max}(w_s, Q)} \quad (2)$$

where $f_{max}(w_s, Q)$ is the maximal value of the function $f(t; w_s, Q)$. If $i(t) = Q_o\delta(t)$ is the Dirac current pulse carrying charge Q_o, then with the aforementioned parameterisation, the resulting electronics response is $ADC^D(t; w_s, Q) = ADC_o \frac{f(t; w_s, Q)}{f_{max}(w_s, Q)}$, the maximal value of which is ADC_o. So this parameterisation implements the electronics gain, i.e. the proportionality between charge input and ADC output, which has been set to: $Q_o = 120$ fC and $ADC_o = 4096$ counts. The electronics response model is parameterized by two variables Q and w_s (eq. 1). They represent the

Quality factor and natural frequency respectively, and their values depend on the values of circuit capacitances and resistances. Both variables are determined by fitting the electronics calibration data [4].

3.2 Charge spreading model

The charge spreading model is based on the theory given in [5]. The spatial and temporal spread of the charge on the resistive layer is governed by the Telegrapher's equation for charge diffusion:

$$\frac{\partial \rho(r,t)}{\partial t} = \frac{1}{RC}\Delta\rho(r,t) \tag{3}$$

where $\rho(r,t)$ is the charge density function, R is the surface resistivity of the layer and C the surface capacitance determined by the spacing between the anode and readout planes. The induced charge on a rectangular pad below the resistive layer can be calculated by integrating the charge density function over the pad area:

$$Q_{pad}(t) = \frac{Q_e}{4} \times \left[erf\left(\frac{x_{\text{high}} - x_0}{\sqrt{2}\sigma(t)}\right) - erf\left(\frac{x_{\text{low}} - x_0}{\sqrt{2}\sigma(t)}\right) \right] \times \left[erf\left(\frac{y_{\text{high}} - y_0}{\sqrt{2}\sigma(t)}\right) - erf\left(\frac{y_{\text{low}} - y_0}{\sqrt{2}\sigma(t)}\right) \right] \tag{4}$$

where $\sigma(t) = \sqrt{\frac{2t}{RC} + \omega^2}$. ω associated to the transverse diffusion term is fixed at 540 µm in 3 cm drift distance, while the longitudinal diffusion is neglected. Here, Q_e is the initial charge after charge multiplication in the amplification region, while (x_0, y_0) is the position of initial charge deposition. The parameters x_{high}, x_{low}, y_{high}, y_{low} are the pad boundaries. Finally, the charge signal function $S(t)$ is obtained as the convolution product of the charge diffusion function (eq. 4) and the derivative of the electronics response function (eq. 2):

$$S(t) \;=\; Q_{pad}(t) \;\circledast\; \frac{d(ADC^D(t))}{dt} \tag{5}$$

3.3 Simultaneous fit of X-ray data waveforms

The signal model (eq. 5) is applied to X-ray data by fitting all the waveforms generated in an X-ray event simultaneously to extract RC and Q_e of the targeted pad. The simultaneous fit is based on χ^2 minimisation, and it uses at least three waveforms within the 3×3 matrix of pads around the leading pad (the scanned pad with the highest signal amplitude) to have enough constraints on (x_0, y_0) position. The fit is performed event by event with the electronics response parameters w_s, Q fixed to the values [4] ($Q = 0.6368$, $w_s = 0.1952$). The model has five parameters:

- t_0 is the time of charge deposition in the leading pad,
- (x_0, y_0) are the positions of initial charge deposition,
- RC of the readout pad - glue - resistive foil network, and
- Q_e is the deposited charge on the resistive foil.

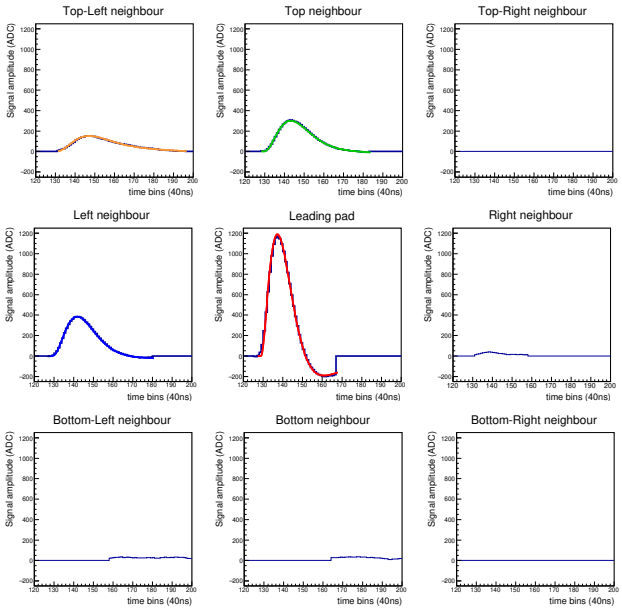

Figure 2: An example of a simultaneous fit of four waveforms of an X-ray generated event [4]. Fit results: RC = (146.6 ± 1.6 ns/mm^2), Q_e = (327.6 ± 1.8) × 10^3e, (x_0, y_0)= (-0.442 cm, 0.352 cm) (w.r.t center of leading pad) , χ^2/Ndf = 1.08.

An example of a simultaneous fit of four waveforms generated in an X-ray event along with their fit results is shown in Figure 2. Upon fitting all the events in one pad, a Gaussian distribution of RC is obtained from the extracted RC values, as shown in Figure 3a. The mean value of the RC distribution over all the events is considered as the global RC value of that pad. Figure 3b shows the fitted parameter Q_e, whose shape is found to reproduce the ^{55}Fe spectrum and thus can be used to extract the gain. The gain can also be extracted from the Q_e distribution by taking into account the number of primary electrons. An energy resolution better than 10% is obtained. Figure 4 shows the RC map and gain distribution of one ERAM. The 2D RC map shows consistent uniformity along the horizontal axis, but global variations of up to 35% are observed across the map. This horizontal uniformity is currently attributed to the DLC foil sputtering process. Recent resistivity measurements have confirmed a correlation between the resistivity patterns of the DLC foil and the features observed in the RC maps.

4. Conclusion

Each module of encapsulated resistive anode of HA-TPC has undergone testing and validation using an X-ray test bench before being installed in the HA-TPC chambers for the T2K experiment. The X-ray test bench characterizes the detectors by scanning each pad individually, enabling precise measurement of gain uniformity and energy resolution, with the latter measured at about 10%.

A detailed physical model has been developed to describe charge dispersion on the resistive Micromegas anode, allowing simultaneous extraction of 2D gain and RC maps from the X-ray data. The model shows excellent agreement with the data, and the uniformity of the RC and gain maps is studied.

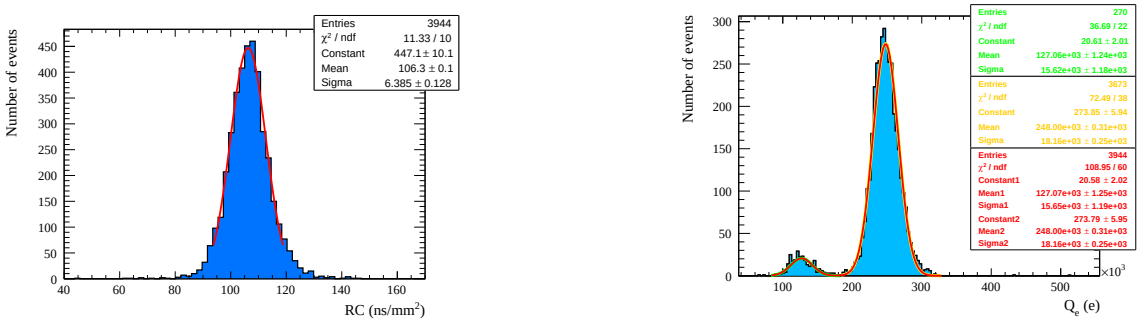

(a) *RC* distribution of one pad. **(b)** Q_e distribution of one pad.

Figure 3: *RC* and Q_e distributions obtained from fitting all events in one pad [4].

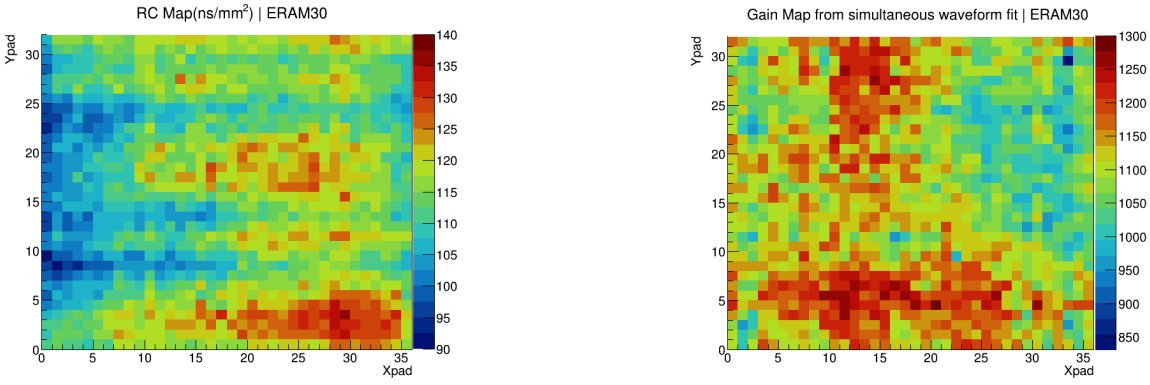

Figure 4: Distribution of *RC* (left) and gain (right) maps extracted from ERAM-30 X-ray test bench data [4].

References

[1] K. Abe et al. (T2K Collaboration), Nucl. Instrum. Methods. Phys. Res. A **659**, 106-135 (2011).

[2] D. Attié et al, *Characterization of resistive Micromegas detectors for the upgrade of the T2K Near Detector Time Projection Chambers*, Nucl. Instrum. Meth. A **1025** 166109 (2022).

[3] P. Baron et al, *AFTER, an ASIC for the readout of the large T2K time projection chambers*, 2007 IEEE Nuclear Science Symposium Conference Record, Honolulu, HI, USA, 2007, pp. 1865-1872, doi: 10.1109/NSSMIC.2007.4436521.

[4] L. Ambrosi et al, *Characterization of Charge Spreading and Gain of Encapsulated Resistive Micromegas Detectors for the Upgrade of the T2K*, Nucl. Instrum. Meth. A **1056** 168534 (2023).

[5] M. S. Dixit, J. Dubeau, J. P. Martin, K. Sachs, Position sensing from charge dispersion in micropattern gas detectors with a resistive anode, Nucl. Instrum. Meth. A518 (2004) 721–727 doi:10.1016/j.nima.2003.09.051